Resveratrol Attenuates Rheumatoid Arthritis Induce Neutrophil Extracellular Traps via TLR-4 Mediated Inflammation in C57BL/6 Mice

Zequan CHEN[1], Guowei XIAO[1], Jian AO[1]

[1]Department of Orthopedics, Wushan County Hospital of Traditional Chinese Medicine, Chongqing, China

Received June 23, 2023
Accepted October 17, 2023

Summary

The objective of this study was to evaluate whether RSV inhibits neutrophil extracellular traps (NETs) that induce joint hyperalgesia in C57BL/6 mice after adjuvant-induced arthritis. A subplantar injection of Freund's complete adjuvant was administered to C57BL/6 mice on day 0 for immunization in the AIA model. Resveratrol (RSV, 25 mg/kg) was administered intraperitoneally once daily starting on day 22 and continuing for two weeks. The effects of mechanical hyperalgesia and edema formation have been assessed in addition to histopathological scoring. Mice were sacrificed on day 35 to determine cytokine levels and PADI4 and COX-2 expression levels. ELISA was used to quantify neutrophil extracellular traps (NETs) along with neutrophil elastase-DNA and myeloperoxidase-DNA complexes in neutrophils. An immunohistochemical stain was performed on knee joints to determine the presence of nuclear factor kappa B p65 (NF-κB p65). AIA mice were found to have higher levels of NET in joints and their joint cells demonstrated an increased expression of the PADI4 gene. Treatment with RSV in AIA mice (25 mg/kg, i.p.) significantly ($P<0.05$) inhibited joint hyperalgesia, resulting in a significant increase in mechanical threshold, a decrease in articular edema, a decrease in the production of inflammatory cytokines, increased COX-2 expression, and a decrease in the immunostaining of NF-κB. Furthermore, treatment with RSV significantly reduced the amount of neutrophil elastase (NE)-DNA and MPO-DNA complexes, which were used as indicators of NET formation ($P<0.05$). This study indicates that RSV reduces NET production and hyperalgesia by reducing inflammation mediated by PADI4 and COX-2. According to these data, NETs contribute to joint pain and resveratrol can be used to treat pain in RA through this pathway.

Key words

Resveratrol • NET formation • PADI4 • Cox2 • Inflammatory mediators

Corresponding author

Z. Chen, Department of Orthopedics, Wushan County Hospital of TCM, No. 277, Guangdong Middle Road, Gaotang Street, Chongqing, China, 404700. E-mail: renruirui79@gmail.com

Introduction

Rheumatoid arthritis (RA) is an autoimmune disease affecting 1-1.5 % of the global population [1]. It manifests itself through joint inflammation and autoantibodies, resulting in pain, cartilage damage, and bone loss [2]. Although the etiology of RA is not fully understood, but it involves genetic, environmental and hormonal factors. An increase in sensitivity to joint pain, hyperalgesia, is the significant symptom of rheumatoid arthritis [3]. Despite advances in RA therapy, patients still face limited pain relief and reduced inflammation due to joint inflammation. The RA model has been used in various animal models to demonstrate the potential role of pro-inflammatory cytokines in the elicitation of joint hyperalgesia [4]. In response to cytokines released by immune cells [5], eicosanoids are produced to stimulate afferent primary neurons.

Neutrophils are also recruited into the joints by cytokines, which act as powerful hyperalgesic mediators, often causing inflammation. Most inflammatory events, including joint pain, are prevented by blocking neutrophil migration to inflamed joints [5]. In addition to

communicating with other cells of the immune system [6], neutrophils are known to release enzymes such as myeloperoxidase (MPO) and matrix metalloproteinases, as well as free radicals derived from oxygen and nitrogen, which cause joint tissue damage [7]. Primary neurons are also sensitized by eicosanoids [5]. NETs, consisting of a DNA matrix associated with extracellular cytotoxic enzymes and proteins, have been demonstrated to be released by neutrophils over the past decade. NETs have been shown to be critical in reducing inflammatory responses. NETs are capable of killing a wide range of bacteria, fungi, protozoa, and viruses [8]. The pathophysiology of a variety of other diseases, such as autoimmune disorders, is also influenced by NETs. Experimental RA is reduced in severity when the enzyme PADI-4 (peptidyl arginine deiminase 4), which plays an essential role in NETosis [9]. The results of several experimental studies on autoimmune diseases showed that NETs mediate tissue damage [10]. NET release of NETs has also been found to magnify the immune response in autoimmunity through recognition of the components as damage-associated molecular patterns (DAMP) [11].

During the past few years, resveratrol (RSV), a polyphenol found in grapes, mulberries, cranberries and walnuts, has attracted considerable attention [12]. RSV shows a wide variety of pharmacological functions, including its antioxidant, antitumor, and anti-inflammatory properties [13]. In addition to modulating enzymes belonging to a variety of classes, RSV also acts to neutralize free radicals by acting on lipoxygenases, cyclooxygenases, and sirtuins [14], which are among its many molecular targets. RSV was also shown to be an effective therapy for arthritis in experimental models by modulating cellular and humoral responses [15]. The efficiency of RSV depends on sufficient levels of active molecules present in the bloodstream and target tissues. Resveratrol has been shown to lower ROS and alleviate RA in animal studies [16]. Meta-analyses of preclinical models suggest that resveratrol can also decrease levels of pro-inflammatory cytokines such as IL-1, IL-6 and TNF-α. Another clinical trial that proved the positive effects of resveratrol on RA patients, where those receiving daily doses of resveratrol supplementation experienced significantly less clinical symptoms and higher serum levels of inflammation [17].

However, there is no evidence that RSV inhibits NET production in joint hyperalgesia of RA. This is despite the fact that NET production is well established during experimental and clinical RA. The present study used an experimental rodent model of RA to investigate whether RSV can inhibit NET in joint hyperalgesia by reducing inflammation through PADI4 and COX-2 in antigen-induced arthritis in C57BL/6 mice.

Materials and Methods

Chemical and reagents

A Myeloperoxidase assay kit from Thermo Fisher Scientific, USA, was used along with Ficoll histopaque 1119/1077 from Himedia labs, China. Reagents and chemicals used in this study were commercially available and of the highest quality.

Animals

Male wild-type C57BL/6 mice weighing 20-25 g were used in the experiments. At the Orthopaedics of Department of Wushan County Hospital, China, all animals were maintained in temperature at 25 °C and provided water and food as needed. The national and international guidelines of the Animal Ethics and care were followed when handling and observing animals. The institutional animal ethics review board approved the study with the approval number ZC-WCH/34-23-34/E/DO.

Antigens

Armour Pharmaceutical Company, Eastbourne, UK, provided bovine serum albumin (BSA, Cohn fraction V) to us as antigens for this study. Using the same method described by Fraenkel-Conrat and Olcott [6], methylated BSA was prepared. The preparations were then lyophilised and stored as lyophilized powders. A sterile intraarticular injection was made by irradiating mBSA with 2.5 megarad and dissolving it to reach the appropriate concentration in the sterile saline prior to injection.

Adjuvants

The antigens in saline were emulsified with 0.5 mg/ml killed Mycohacieriuni butyricum in the complete Freund adjuvant in equal volume, and added to a glass vial containing 1.0 ml of saline. A Bordetella pertussis (2×10^7) organism was injected intraperitoneally into the mice.

Immunization of mice with mBSA and treatment protocol

Antigen-induced arthritis (AIA) is induced using the same method as previously described [18], but with

minor alterations. A subcutaneous injection of 500 g of methylated bovine serum albumin was used in 0.2 ml of Freund's adjuvant (1 mg/ml of Mycobacterium tuberculosis) and a complete Freund's adjuvant (0.1 ml) to sensitize mice on day 0. A similar preparation was used to stimulate mice on day 7. A similar injection was given to control mice, but without mBSA. It was recommended to administer a second immunization, as mentioned above, 14 days after initial sensitization. The first challenge was used as an inducer by administering mBSA (100 µg/cavity) intraarticularly into either the right or both knee joints, respectively, on the 21st day after the second immunization. Similarly, to the first challenge, the mice were again challenged on day 28.

A total of 48 mice with 12 mice in each group were randomly assigned to the following four groups on day 21 after the first challenge. Group 1: normal control (untreated). Group 2: arthritic control (vehicle-treated, AIA). Group 3: RSV (15 mg/kg, i.p.) was given to arthritis-prone mice. Group 4: RSV (25 mg/kg, i.p.) was given to arthritis-prone mice. As part of the study, resveratrol was administered intraperitoneally once daily from day 22 to day 35 (two weeks) with a mixed solution of 25 mg/kg body weight of resveratrol (15 or 25 mg/kg, initially dissolved in 7 % DMSO and 35 percent PEG 300, and subsequently added to normal saline). The mixed solution was administered intraperitoneally to AIA mice.

Autopsies and histology

A 70 % ethanol solution was used to clean the knees on day 36, under slight ether anaesthesia. To quantify NETs, it is necessary to open the knee joints and wash them with phosphate buffer saline to clean them. Aspirated fluids were used for further analysis and PADI4 expression after treatment.

A cervical dislocation was used to sacrifice mice and a sample of blood (2 ml) was collected from each animal. The patellar tendon was incised through a transverse incision and sterile conditions were used to open the knee joints, removing the hind legs, and skinning them. An aerobic and anaerobic leg culture was performed for one week in nutrient broth and Brewer's medium, respectively. There was no sign of bacterial growth on the horse blood agar after placing one drop of the nutrient broth medium on it. Formaldehyde and nitric acid were used to decalcify the legs after initial fixation with 10 % phosphate buffer formalin. A series of alcohol baths of 70 to 90 % was then applied to dehydrate them for 2-3 h, followed by 24 h in absolute alcohol after they had been dehydrated. In this case, the sample was first cleared in chloroform and then embedded in paraffin wax at 60 °C, where serial sections were stored for immunostaining procedures.

Evaluation of articular hyperalgesia

For evaluation of femur-tibial joint hyperalgesia after treatment, as described previously [19], an electronic von Frey test was performed. We applied increasing force perpendicularly to the plantar surface of the hind paw, causing the femur-tibia joint to flex and then withdraw the paw. An electronic pressure meter was used to record the force applied to the paw when it was withdrawn.

A blinded investigator conducted several repetitions of the test until three consecutive measurements with variance greater than one gram were obtained. A mechanical threshold is measured in grams, and a reduction in the threshold can be seen as a sign of hyperalgesia. A calliper was used to measure the thickness of the knee joints in millimeters. During the experiment, the diameter was measured on days 22 (basal) and 36 (therapy), and the result was expressed as the mean and the difference between the two diameters (Δmillimeters).

Cytokine measurements

The knee joints of the animals were isolated and homogenised in 500 ml of protease inhibitor-containing buffer after terminal anaesthesia. TNF-α and IL-1β levels were determined by ELISA (R&D Systems, USA) using conjugated antibodies as previously described [20]. Each cytokine is expressed in pg/mg.

Our subsequent experiments were conducted with RSV (25 mg/kg, i.p.) based on findings of articular hyperalgesia (mechanical threshold and reduction of knee joint thickness) and cytokine levels. It appears to be poorly absorbed when administered intraperitoneally at a lower dose (15 mg/kg) due to its low bioavailability. Hence, we selected a higher dose of RSV (25 mg/kg).

Neutrophil isolation and collection of cell-free supernatants containing NETs

The neutrophils of different experimental animals were separated by using the density gradient method. Aspirated fluids from the entire articular joints were placed onto Ficoll Paque Premium (Sigma Aldrich, China) using the Ficoll histopaque 1119/1077 density gradient technique. Aspirated joint samples (5 ml) were layered over Granulosep 1119 and Hisep 1077 to achieve

a density gradient. The sample was centrifuged for 2 min at 700× g. The desired volume was obtained by pooling joint samples within each group. HBSS was used to separate neutrophils. Then they were carefully resuspended in serum-free DMEM. Cell pellets were resuspended in chilled phosphate buffered saline and washed for five minutes. RPMI-1640 + 2 % fetal calf serum culture medium was then used to resuspend the granulocyte pellets. Cell viability was greater than 94 % under different experimental conditions. Cell purity was also confirmed using trypan blue (0.4 %) in PBS (phosphate buffered saline). The composition was measured by freezing cell-free supernatants at 80 °C.

Observation of NETs Release from neutrophils

Hoechst staining was used to visualize the release of NETs. To stain viable neutrophil nuclear DNA, 5 µmol/l of Hoechst 33342 (Invitrogen, USA) were applied to each well and incubated for 10 min in 5 % CO_2 at 37 °C. We diluted Hoescht 33342 stock solution in PBS to 1:2000 and added enough solution over the cells (500 µl per well in a 48-well plate) and then incubated the cells for 20 min at room temperature. To remove the excess stain from the cells, the cells were gently washed three times with phosphate buffer saline. The wells were excited with laser excitation and emission wavelengths at 340 nm and 471 nm, respectively, before microscopy. An Olympus IX70 inverted fluorescence microscope with UV filter (excitation wavelength 340 nm) was used to image neutrophils. ImageJ software (http://rsbweb.nih.gov/ij/) was used to composite images taken with a DP72 digital camera (Olympus) at magnification ×100.

A scanning electron microscope was used to observe and photograph NETs in greater detail. Once cells had been incubated, the medium had been removed and 3 % glutaraldehyde in phosphate buffer saline for one hour at 37 °C. After dehydrating for five minutes with increasing alcohol concentrations – 45 %, 65 %, 85 %, and 100 % – ensure the cells were completely dried. The coverslips were coated with carbon sputter before viewing the cells under the Hitachi S3400N scanning electron microscope [21].

Neutrophil elastase (NE)-DNA and MPO-DNA complexes to quantify NET formation using ELISA

Based on the association of MPO with NETs [22], MPO-DNA capture ELISA was used for the detection of pre-existing NETs in cell-free supernatants obtained from joint samples. It was used to break DNA-MPO particles in the NETs and obtain smaller particles for the DNA-MPO assay by treating aspirated fluids from joint samples with 500 U/ml of MNase (micrococcal nuclease) from Staphylococcus aureus. A 96-well plate (dilution 1: 400 in 30 ml) was coated with 5 mg/ml anti-MPO mAb (Millipore) overnight at 4 °C for the capture antibody. The plate was then washed three times with PBS (300 µl each) before coating with 1 % bovine serum albumin. After applying MNase to the joint samples, 20 µl of each MNase treated sample was added to the wells, along with an incubation buffer that contained a peroxidase-labelled anti-DNA mAb (Cell Death ELISA PLUS, Roche; 1:30 dilution). The plates were shaken for two hours at 37 °C. A total of three washes (30 µl each) followed by 100 µl of peroxidase substrate. At 430 nm, the absorbance was measured after a 20-minute incubation in the dark at room temperature. An increase in absorbance above control is used to determine soluble NET formation values. OD was measured using a Synergy H1MF microplate reader (USA) at 410 nm and 470 nm. Finally, we divided the sample values OD 410-470 by the positive control OD 410-470 values to obtain the OD 410-470 index.

NE-DNA interactions were measured in cell-free supernatants as previously described [23]. Plasma neutrophil elastase-DNA complexes were measured by Sandwich ELISA to detect NETs. Microtiter plates with 96 wells were coated overnight with the capture antibody against neutrophil elastase (100 µl/well; cat. ab68672, abcam) diluted in carbonate-bicarbonate buffer (pH 9.4, cat. No. C3041, Sigma-Aldrich, USA; 1:800) at 4 °C. The samples were blocked with bovine serum albumin (5 % bovine serum albumin, 300 µl per well), after which we added the joint samples (100 µl per well) and incubated with peroxidase conjugated antibodies for DNA detection (The Cell Death Detection ELISAplus Kit, Roche). The percentage increases in absorbance above the control represent soluble NET formation. A Synergy H1MF microplate reader (BioTek, USA) was used to measure the optical density at 450 and 490 nm. Finally, we divided the OD450-490 values from the sample by the positive control OD450-490 values OD450-490 to get the OD 450-490 index.

Reverse transcription-polymerase chain reaction assays

A Qiagen kit (Qiagen, Germany) was used to extract RNA from the cell-free supernatant of articular joint samples to evaluate the expression of the PADI4 and

COX-2 genes. A Trizol reagent (Thermo Fisher Scientific) was used to extract total cellular RNA. Quantification of the amplicons was performed using the SYBR-green fluorescence system (Applied Biosystems, USA). The primers used were the following: GAPDH forward: 5-AAGTTCGGAGAGATTAG-3, reverse: 5-GGTTACCTTGTTACGACTT-3; PADI4 forward: 5-GACCTAATAGTTACCGAA-3; reverse: 5-ATCCTA-AGGCCCAGGGTAC-3; COX-2 forward: 5-GGATTC-CGCCGAATCCAG-3; reverse: 5-AACTTACGGGAG-CCAATATTC-3.

Western blot analysis of PADI4 and COX-2 expression in articular aspirated fluids

An articular joint supernatant was lysed with a lysis buffer to obtain total protein. The lysates were centrifuged at 4 °C for 1 min after 30 min on ice. We used Pierce Biotechnology, Inc.'s bicinchoninic acid (BCA) assay reagents to assess the protein content. We separated the protein (40 µg) on 12 % SDS polyacryl-amide gels and transferred it onto polyvinylidene difluoride membranes. The membrane incubation was followed by blocking with 5 % non-fat milk 5 %. We used anti-PADI4 rabbit polyclonal antibody (1:800 dilutions; Santa Cruz Biotechnology, USA). Rabbit anti-COX-2 IgG (1:1000 dilution, Cell Signaling Technology, USA), and the anti-β-actin mouse monoclonal antibody anti-β-actin (1:800 dilution) at room temperature for 3 h. Incubation of the membranes with rabbit anti-mouse IgG (1:2000 dilution) and mouse anti-rabbit IgG (1:2000 dilution) was performed at 37 °C with horseradish peroxidase (HRP) conjugated secondary antibodies. An ECL detection kit (Pierce Biotechnology) was used to detect the signals. ImageJ software was used to quantify protein band intensity. Normalisation of relative protein levels was performed using β-actin.

Assessment of nuclear factor-kappa B p65 expression

In both treated and untreated groups, NF-κB/p65 polyclonal antibodies (1:200 dilution) were used for immunohistochemistry staining of knee joint sections, followed by washing and incubation with horseradish peroxidase (HRP) conjugated secondary antibodies for 30 min. An increase in brown color was observed in synovial tissue when the NF-kB p65 protein was detected under light microscopy. The Leica Biosystems slide analysis software was used to calculate the mean expression area percentage of NF-kB from 8 random fields.

Statistical analysis

Data are expressed as mean + standard error of the mean (SEM). Data normality was determined using the Kolmogorov-Smirnov (KS) test, and all data had a normal distribution. ANOVA was used to compare the mean of different groups, followed by the Tukey-Kramer multiple comparison test. These statistical tests were conducted with Graph Pad Prism 9.5 (Graph Pad Software Inc, San Diego, California, USA). Statistical significance was determined by a P value of less than 0.05.

Results

Effect of RSV on Articular hyperalgesia

To evaluate the effects of RSV on hyperalgesia of the joints, to determine whether administration of RSV could inhibit hyperalgesia. Compared to the control group, there was a significant reduction in the mechanical threshold, indicating momentous induction of mechanical hyperalgesia. It improved significantly ($P<0.05$) improved after RSV (25 mg/kg, i.p.) administration relative to AIA group.

In addition, the effects of RSV on joint swelling were determined and analysed. There was a significant increase in joint swelling around the knee joint indicating a momentous induction of hyperalgesic activity in AIA mice compared to the control group. It decreased significantly ($P<0.05$) decreased after oral administration of the RSV dose (25 mg/kg) compared to the AIA group (Fig. 1).

Effect of RSV on cytokine production mediated through Toll-like receptors 4 and 9 in AIA-induced hyperalgesia

Toll-like receptors, TLRs, which coordinate the release of hyperalgesic cytokines, cause inflammatory hyperalgesia, as previously demonstrated [24]. The purpose of this study is to determine the mechanism by which RSV effects local hyperalgesia mediated through TLR receptors. It is apparent that AIA-induced hyperalgesia affects the release of these cytokines through the activation of the TLR-4 and TLR-9 receptors, as evidenced by low concentrations of TNF-α and IL-β in synovial fluid after RSV treatment (25 mg/kg, i.p., Fig. 2). There was a significant reduction in the nociceptive threshold demonstrated by the reduced TNF-α and IL-1β levels when treated with the RSV dose (25 mg/kg) (Fig. 2), indicating that TLR-4 and TLR-9 receptors play a role in the reduction of nociceptive threshold. According to these findings, resveratrol administration improved AIA in mice as well as inflammatory responses to joint injury.

Effects of RSV on the Release of NETs

We further demonstrated and confirmed NET release by nuclear staining with Hoechst 33342 and scanning electron microscopy in isolated neutrophils obtained from various experimental animals. A significant increase in the release of NET was observed in isolated neutrophils from AIA mice (Fig. 3) compared to the control group. We found that RSV (25 mg/kg, i.p.) decreased considerably ($P<0.01$) the release in joint samples (Fig. 3) compared to the AIA group. A scanning electron microscope (Fig. 3) also confirmed these findings. NET production was significantly high in the AIA model group compared to the control ($P<0.05$). NET values were considerably lower after RSV treatment with RSV (25 mg/kg, i.p.) relative to the AIA group ($P<0.05$; Fig. 4). According to the above findings, the neutrophil infiltration, survival, and NET release of the AIA model can be affected by resveratrol administration.

Effects of RSV on neutrophil elastase (NE)-DNA and MPO-DNA complexes to quantify NET formation using ELISA

Our detection of MPO-associated DNA by ELISA further confirmed our fluorescence microscopy experiments and quantified NET formation. NET formation was calculated as a percentage by normalizing the optical density measurements to those of the negative control. Based on these NET-specific assays, we found that AIA model groups produced NETs with a large increase in MPO-DNA complexes relative to the control group, while RSV treatment with RSV (25 mg/kg, i.p.) produced only minimal increases in NET percentage. The MPO-DNA ELISA was used to detect NETs in joint fluid samples, because MPO and DNA in the scaffold of NETs are associated with each other. Figure 5 shows the results.

Similar results were also obtained using the neutrophil elastase (NE)-DNA complex in which the NETs in AIA model group showed a significant increase ($P<0.01$) that were attenuated after RSV treatment with RSV (25 mg/kg, i.p). This suggests that NETs contribute to increased permeability in AIA-induced rheumatoid arthritis. In addition, we were able to localize markers of NETs, such as NE and MPO (Fig. 4) in both treated and untreated groups. These markers are located exactly at the location of the NETs, as shown in Figure 5. According to the above findings, RSV (25 mg/kg, i.p.) inhibited the formation of NET, thus exhibiting anti-arthritic effects. AIA-induced arthritis seems to be increasing the number of neutrophil cells and the expression of NE and MPO markers, but treatment with RES leads to a decrease in the number and markers' expression.

Effects of RSV on PADI4 and COX-2 gene expression using RT-qPCR

To confirm the presence of NETs in neutrophils isolated from treated and untreated mice, we quantified the expression of PADI4 and COX-2. The expression of the PADI4 and COX-2 genes also increased in AIA animals that migrated to the articular joint, indicating an association between PADI4 and COX-2 expression and NET production (Fig. 6). Treatment of AIA animals with RSV (25 mg/kg) considerably ($P<0.05$) reduced PADI4 or COX-2 expressions when compared to the AIA group. We found that resveratrol antagonized neutrophil migration and inflammation by inhibiting PADI4 and COX-2. The results of these studies indicated that resveratrol inhibited neutrophil migration, chemotaxis, and inflammation through the inhibition of PADI4 and COX-2 expression levels.

Effects of RSV on PADI4 and COX-2 expressions using Western blot analysis

Furthermore, Western blot analyses were then performed to determine the levels of expression of PADI4 and COX-2 expressions in aspirated fluids to further confirm the role of NETs in the expression of PADI4 and COX-2 in antigen–induced arthritis in mice as previously published. AIA animals showed increased expression of PADI4 and COX-2 in their articular joints, suggesting that increases in NET production may be linked to these genes (Fig. 7). Treatment of AIA animals with RSV (25 mg/kg) considerably ($P<0.05$) reduced PADI4 or COX-2 expressions when compared to the AIA group.

Analysis of the expression of nuclear factor kappa B p65

Immunohistochemical examination of the synovial tissues of the normal group showed no evidence of the expression of NF-κB p65, in contrast to the expression observed in the synovial tissues of the arthritis control group. As expected, the RSV group (300 mg/kg) slowed down NF-B p65 expression similarly to the normal group (Fig. 8).

Discussion

For the first time, resveratrol has been tested in mice infected with antigens to determine whether it influences NET formation. The formation of NETs aids

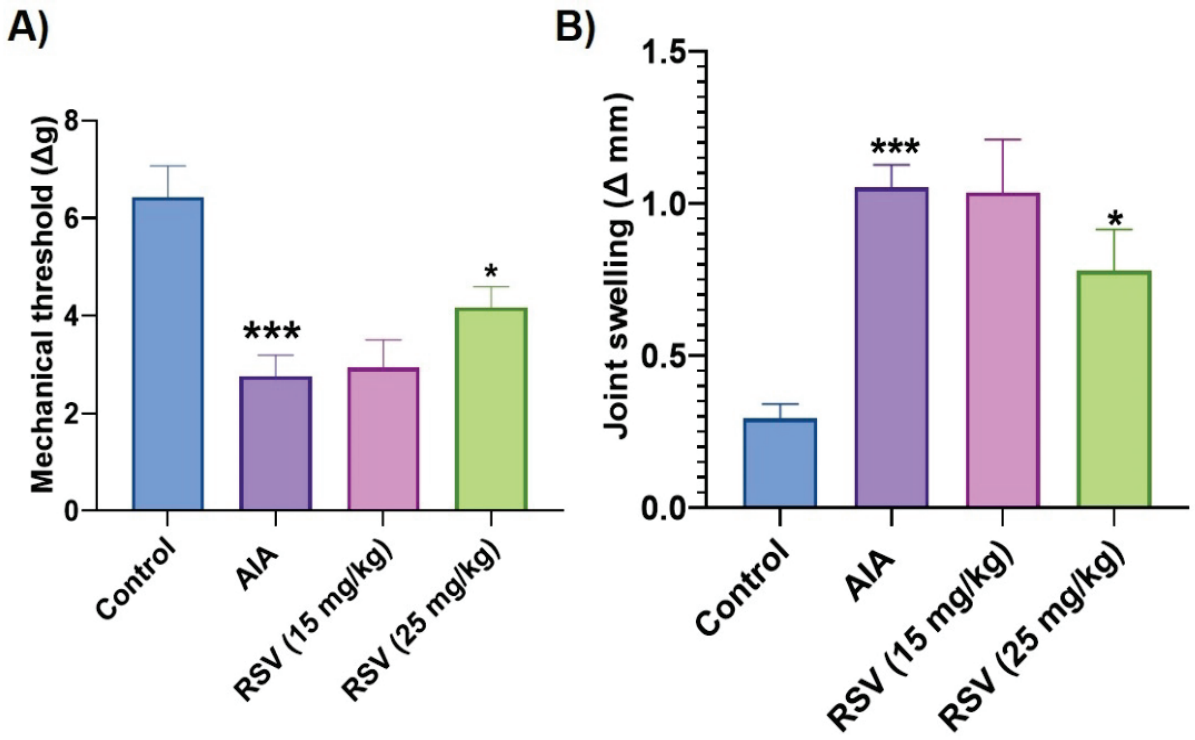

Fig. 1. Alleviation of articular hyperalgesia in adjuvant-induced arthritis following the treatment of resveratrol in mice. (**A**) Administration of resveratrol attenuates AIA-induced mechanical hyperalgesia in mice. (**B**) Joint swelling was assessed by measuring ankle joint diameter. Values are the mean ± standard error of the mean (SEM). *** P<0.001 when comparing antigen induced arthritis treated with the control group. * P<0.05 when comparing antigen-induced arthritis group with RSV (25 mg/kg, i.p.) group.

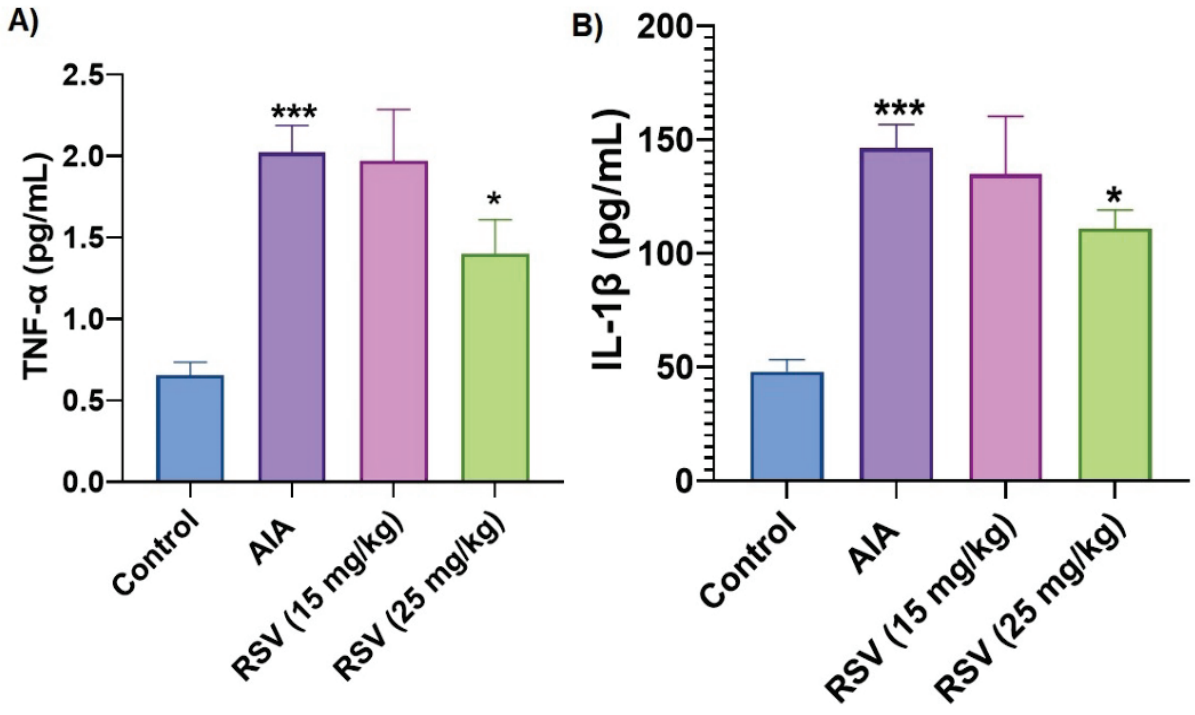

Fig. 2. Alleviation of inflammatory cytokines in adjuvant-induced arthritis following the treatment of resveratrol in mice. (**A**) TNF-α was quantified in joint samples of mice in AIA treated and RSV (15 or 25 mg/kg, i.p.) groups. (**B**) IL-1β was quantified in joint samples of mice in AIA treated and RSV (15 or 25 mg/kg, i.p.) groups. Values are the mean ± standard error of the mean (SEM). *** P<0.001 when comparing antigen induced arthritis treated with the control group. * P<0.05 when comparing antigen-induced arthritis group with RSV (25 mg/kg, i.p.) group.

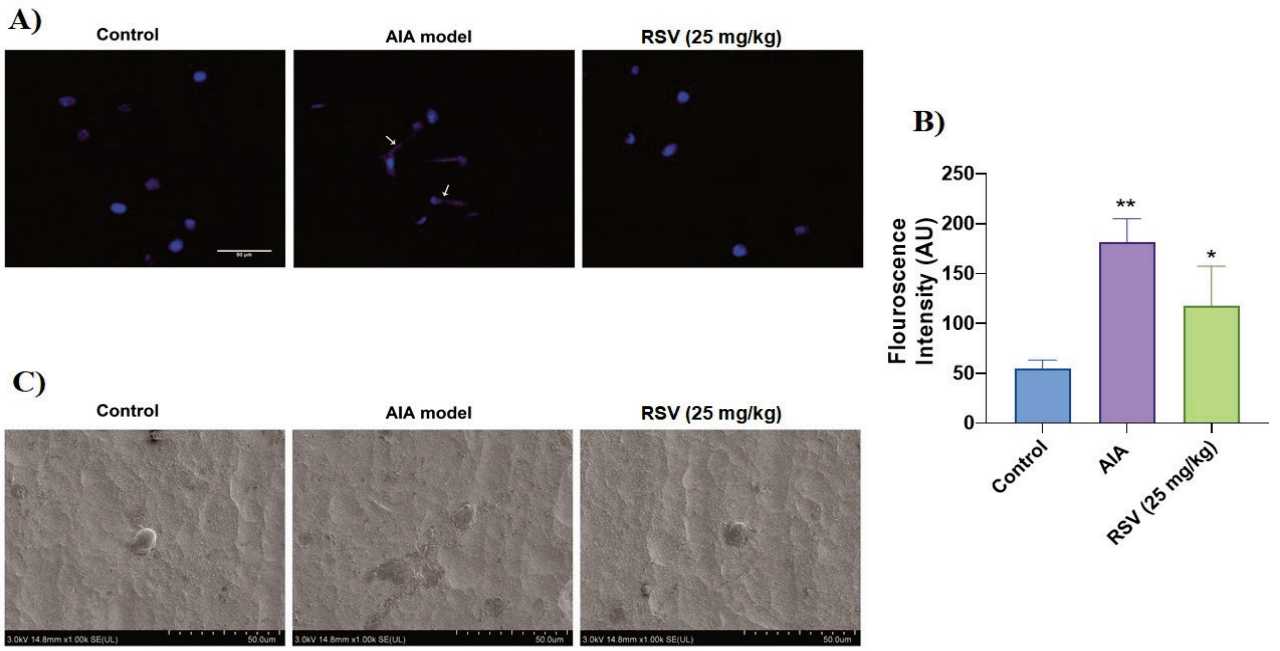

Fig. 3. Representative images of neutrophil extracellular traps. (**A**) Fluorescence microscopic images (magnification 200×) and (**B**) quantification of NETs. (**C**) Scanning electron microscope images. Arrow indicate the NETs (n=3; with duplicate each time). Values are the mean ± standard error of the mean (SEM). ** P<0.01 when comparing antigen induced arthritis treated with the control group. * P<0.05 when comparing antigen-induced arthritis group with RSV (25 mg/kg, i.p.) group.

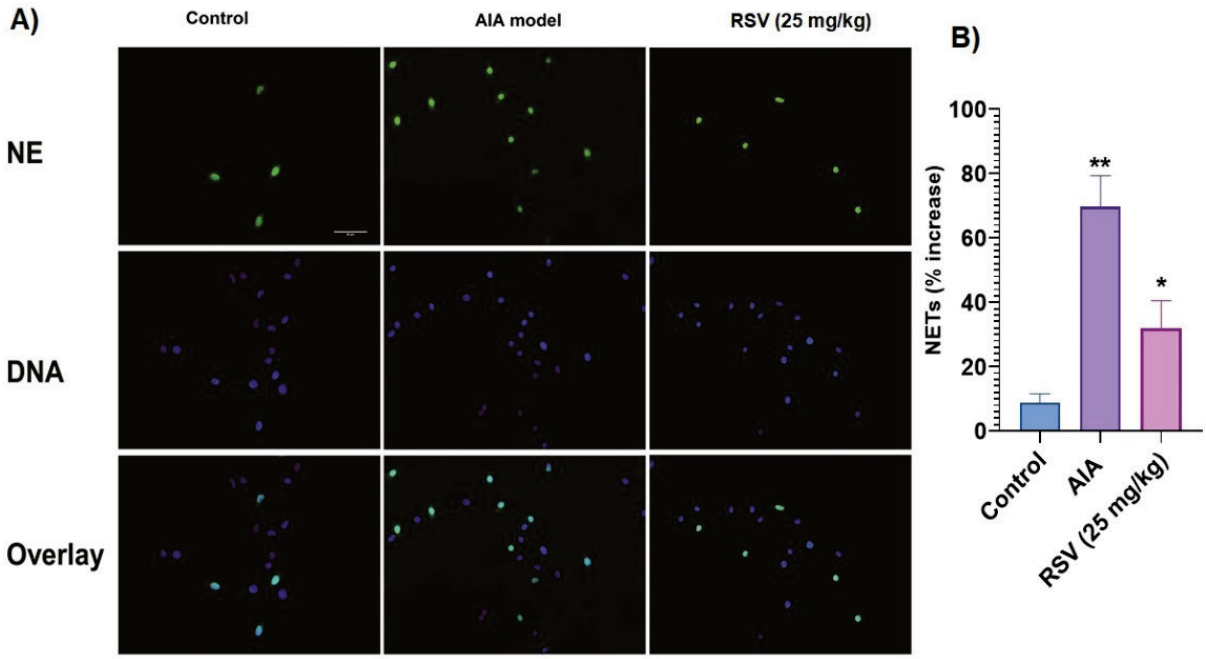

Fig. 4. Quantification of NET in joint samples after RSV treatment. (**A**) NE-DNA ELISA was used to quantify NET formation in the plasma of mice treated with RSV (25 mg/kg, i.p.). (**B**) Quantitative analysis of NETs percentage release after treatment with RSV (25 mg/kg. i.p.). Values are the mean ± standard error of the mean (SEM). *** P<0.001 when comparing antigen induced arthritis treated with the control group. *P<0.05 when comparing antigen-induced arthritis group with RSV (25 mg/kg, i.p.) group.

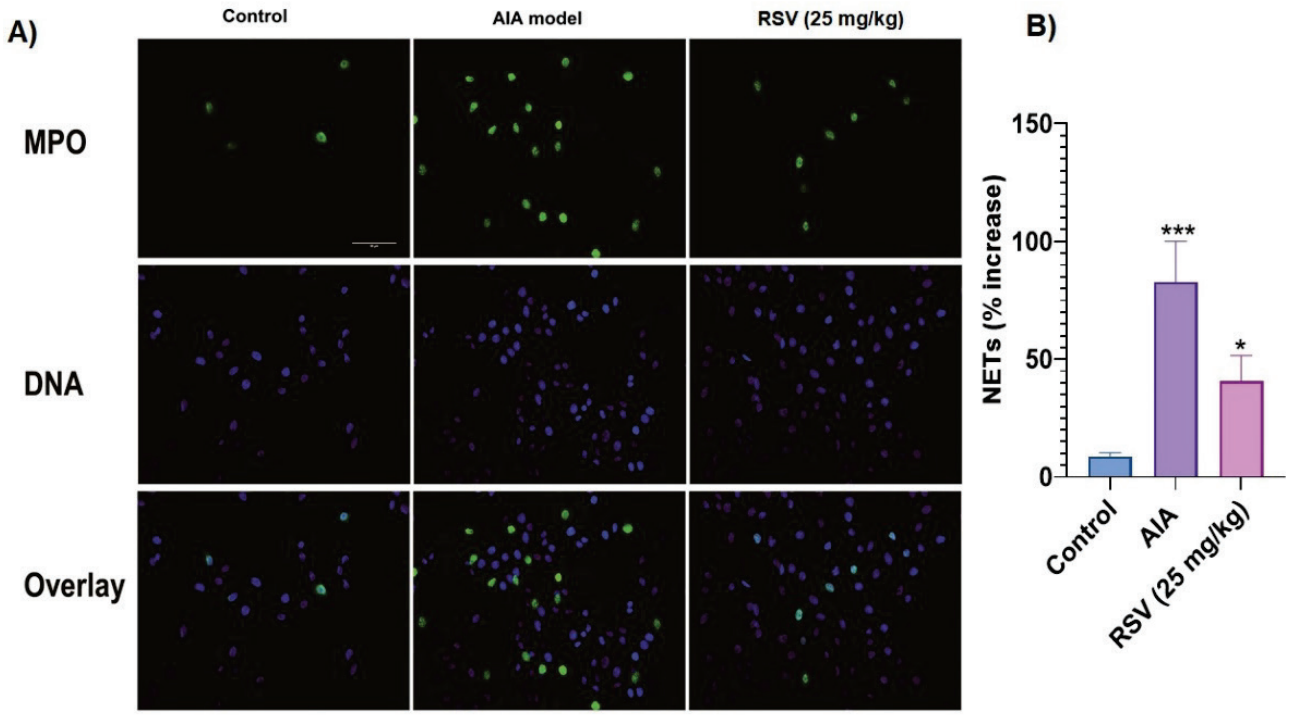

Fig. 5. Quantification of NETs in joint samples. (**A**) MPO-DNA ELISA was used to quantify NET formation in the plasma of mice treated with RSV (25 mg/kg, i.p.). (**B**) Quantitative analysis of NETs percentage release after treatment with RSV (25 mg/kg. i.p.). Values are the mean ± standard error of the mean (SEM). *** P<0.001 when comparing antigen induced arthritis treated with the control group. * P<0.05 when comparing antigen-induced arthritis group with RSV (25 mg/kg, i.p.) group.

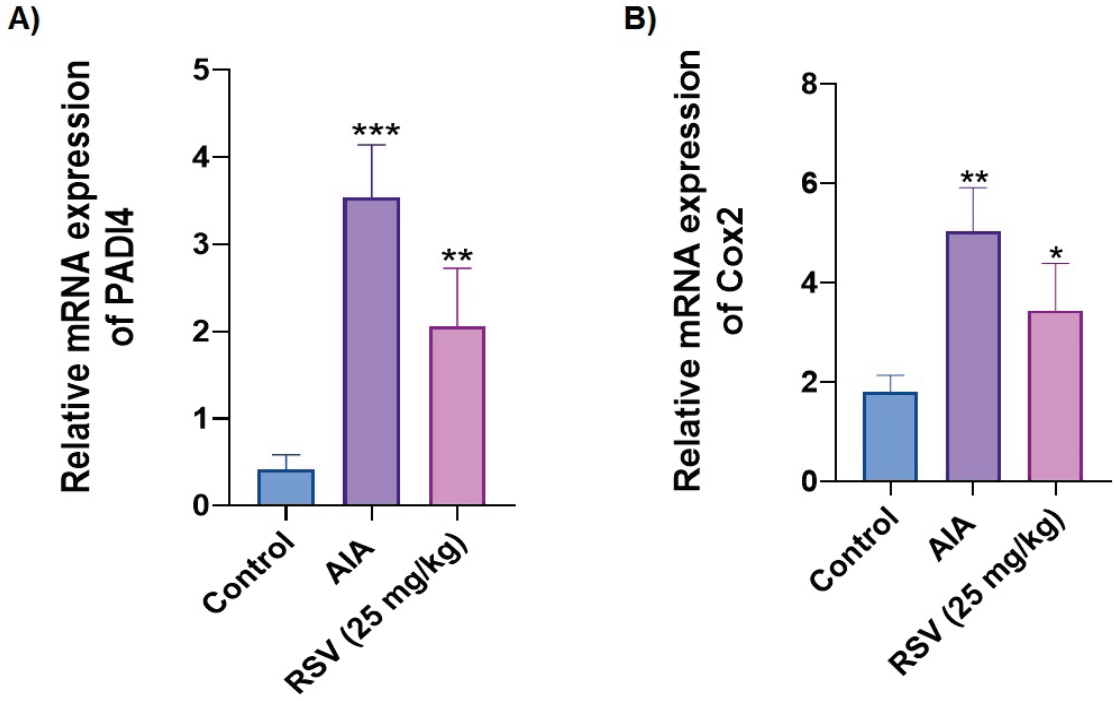

Fig. 6. Expression and nuclear localization of PAD4 and COX-2 in joint samples. (**A**) The mRNA levels of PAD4 in joint samples following RSV treatment (25 mg/kg, i.p.). RT-qPCR analysis was performed with RNA isolated from the joint sample. (**B**) The mRNA levels of COX-2 in joint samples. RT–qPCR analysis was performed with RNA isolated from the joint samples following treatment with RSV (25 mg/kg, i.p.). Values are the mean ± standard error of the mean (SEM). *** P<0.001 & ** P<0.01 when comparing antigen induced arthritis treated with the control group. ** P<0.01 & * P<0.05 when comparing antigen-induced arthritis group with RSV (25 mg/kg, i.p.) group.

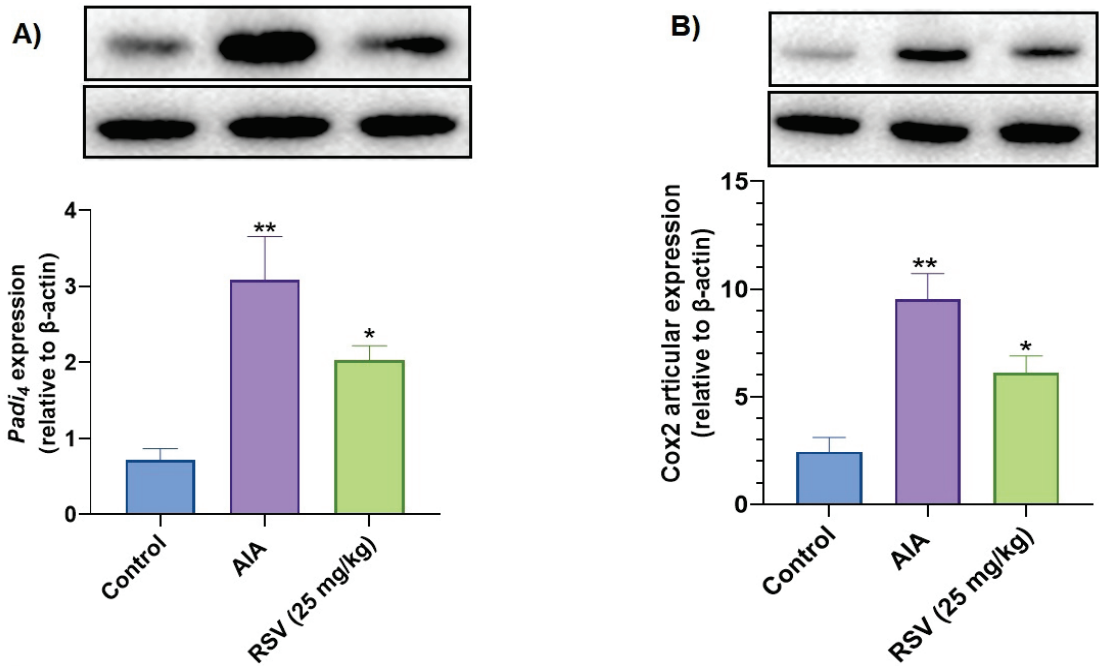

Fig. 7. Western blot analysis of gene expression of PAD4 and COX-2 in joint samples. (**A**) PAD4 expression levels in joint samples following RSV treatment (25 mg/kg, i.p.). (**B**) COX-2 expression levels in joint samples. Values are the mean ± standard error of the mean (SEM). ** P<0.01 when comparing antigen induced arthritis treated with the control group. * P<0.05 when comparing antigen-induced arthritis group with RSV (25 mg/kg, i.p.) group.

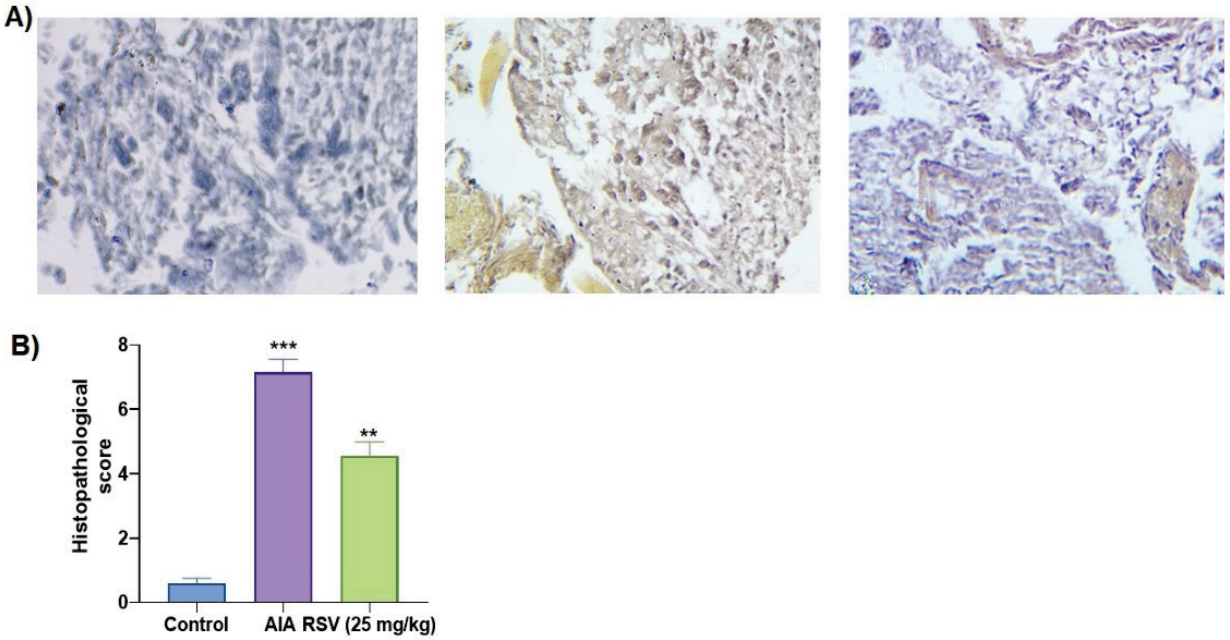

Fig. 8. Immuno-histochemical analysis of NF-κB p65 expression (magnification 400×) in synovial tissues of (**A**) normal group, adjuvant-induced arthritis (AIA) group, resveratrol (RSV) (25 mg/kg i.p.). (**B**) Histopathological score representation. *** P<0.001 when comparing antigen induced arthritis treated with the control group. ** P<0.01 when comparing antigen-induced arthritis group with RSV (25 mg/kg, i.p.) group.

in the fight against infection. However, excessive NET production may compromise cell function and cause tissue damage. NETs are used for a number of autoimmune diseases, including RA. NETs appear in joint tissue lesions due to RA [25]. The release of cytokines stimulates COX-2 expression. It was first determined whether NETs could be induced in AIA mice when mBSA was injected into their joints. Several

characteristics of this model resemble those of rheumatoid arthritis, including edema, histopathological changes, increased pro-inflammatory cytokine production, and joint hyperalgesia [26]. The AIA model has been shown to increase NET production. There is an association between NET levels and PADI4, an enzyme involved in NET release [27].

Recent studies have shown that resveratrol may have health benefits in a variety of diseases, such as obesity, diabetes, cardiovascular disease, inflammation of the bowel, and cancer [28,29,30]. In fact, numerous studies have shown that resveratrol directly affects lymphocytes, macrophages, and neutrophils, which play crucial roles in innate and adaptive immunity [31]. According to our study, resveratrol inhibited joint-synovial neutrophil infiltration in AIA mice. Active neutrophils release DNA-histone complexes and proteins that form extracellular neutrophil traps, which serve as key components of their innate immune response [32]. Neutrophil NET generation is downregulated by resveratrol in patients with severe COVID-19, according to a recent study [33]. According to our data, the AIA mouse model also demonstrated the same result.

NET concentrations and joint edema were reduced in AIA mice treated with RSV (25 mg/kg, i.p.). RSV (25 mg/kg, i.p.) not only inhibits PADI4, but also inhibits NETs through DNase degradation, leading to NETs degrading themselves. NET-associated hyperalgesia, synovitis, and joint edema, which have been reported in association migration of neutrophils, were reduced in AIA mice after RSV treatment. The animals also showed reductions in joint hyperalgesia, edema, and synovitis events. In summary, our results add to our understanding of the mechanisms underlying the antiarthritogenic and anti-hyperalgesic effects of RSV on migratory neutrophils in AIA, triggered by the release of NET. There was a significant reduction in the decrease in the nociceptive threshold in the mice treated with RSV (mechanical hyperalgesia) induced by joint challenge, confirming that joint hyperalgesia can be effectively mediated by NET and, therefore, are effective at reducing pain during joint stimulation. Furthermore, we found that PADI-4 inhibitors reduced joint inflammation in arthritis animals, corroborated our findings that NET production was also elevated in the collagen-induced arthritis model and that NET production was also elevated in the collagen-induced arthritis mouse model [9].

The main cause of the production of eicosanoids during inflammation is the activation of COX [34]. There is no doubt that PGE2 is one of the most important players in sensitizing neurons with high levels of sensitivity among eicosanoids [5]. COX inhibitors have been shown to be clinically effective in the treatment of inflammatory hyperalgesia as a result of their ability to inhibit COX. Several studies have revealed that COX-2 activation is an outcome of cytokines that are released during inflammation, including inflamed joints, and which are connected with COX-2 induction [35]. Our research was motivated by the possibility that NET could cause joint hyperalgesia through the mechanisms described above. First, we demonstrate that NETs induce TNF-α and IL-1β, which mediate joint hyperalgesia. A consistent finding was that AIA animals treated with RSV (25 mg/kg, i.p.) had reduced hyperalgesia, indicating that these cytokines may be involved in the cause of hyperalgesia, as shown by the decreased pain thresholds in these animals. The results of our study also confirmed that RSV treatment of mice reduced COX-2 expression in the joints, confirming that COX-2 is involved in NET-induced hyperalgesia, and therefore inhibiting NET-induced joint hyperalgesia. Several studies have reported that RSV is capable of inhibiting cellular infiltration, synovial hyperplasia, and cartilage erosion when injected into the synovium [36]. Furthermore, it was previously that RSV inhibits neutrophil infiltration of neutrophils by downregulating the expression of chemokines [37].

Therefore, NETs are released from the nucleus, which then allows the enzymes elastase and MPO to move into the nucleus and facilitate the decondensation of chromatin by releasing them from the nucleus. A granular or cytosolic protein is present in the cytosol, which allows DNA to be transported to the cytosol, where it mixes with other proteins in the cytosol [11]. This study also showed similar results, where NETs were released in AIA models with increased neutrophil elastase as well as MPO-DNA complexes, suggesting the existence of NETs. Interestingly, RSV can significantly inhibit these results when administered intraperitoneally at a dose of 25 mg/kg. There are also other antioxidant flavonoids that inhibit NET release. There are several compounds that inhibit the formation of NETs, including epicatechin, catechin hydrate, and rutin trihydrate [38]. Several studies have shown that quercetin and luteolin can prevent the formation of NETs in patients with malignant oral disease [39]. Despite the fact that microbicidal structures were originally described as NETs, an increasing number of studies have shown that

NETs are caused by adverse effects on a variety of tissues in addition to microbicidal effects. A study by Jorgech and Kubes in 2017 shows that NETs will exacerbate inflammatory processes in rheumatoid arthritis, chronic lupus erythematosus, diabetes, cancer, and thrombosis [11]. Therefore, to treat diseases exacerbated by NETs, it is imperative to seek alternatives to traditional therapeutic treatments. There is strong evidence from our study and from other studies, that resveratrol is highly effective at inhibiting NET release and the microbicidal enzymes they produce.

Furthermore, NF-κB regulates cytokine transcription to counteract pro-inflammatory conditions [40]. As revealed in the current study, arthritis induction increased serum levels of TNF-α and IL-1β and increased expression of NF-κB p65. As a result of RSV treatment, there was a decrease in estimated levels of proinflammatory cytokines and NF-kB p65 expression. According to the study published by Lu *et al.*, similar results were reported. It has been shown that RSV reduces inflammation in arthritis-suffering rats by decreasing serum levels of pro-inflammatory cytokines [41]. Furthermore, previous *in vitro* studies have shown that RSV suppresses NF-κB signaling by synovial fibroblasts as well as articular chondrocytes in articular cartilage [42]. Despite this, after RSV administration, plasma levels of TNF-α and IL-1β returned to normal. RSV-treated mice showed a decrease in NF-B p65 expression compared to untreated mice, where this level was nearly unchanged from the untreated group. It was found that the normalized effect was due to the anti-inflammatory effects of RSV.

Conclusions

As a result of our findings, we report for the first time that, in the AIA arthritis model, NETs released from joints are found to be responsible for inducing the release of TNF-α and IL-1β, possibly through toll-like receptors, concluding that the release from joints causes the release of TNF-α and IL-1β. Subsequently, these cytokines cause an increase in the expression of COX-2, which contributes to hyperalgesia as a result. Therefore, it is possible to consider inhibition of NET production of NETs in analgesic therapies for inflammatory pain. The results of these experiments clearly demonstrate that RSV administration significantly alleviates joint damage, since this was evident from the joint volume decrement, histopathological and immunohistochemical examinations, and enhanced inflammatory and NET biomarkers, as well as the decrease in the joint volume.

Conflict of Interest

There is no conflict of interest.

References

1. Silman AJ, Pearson JE. Epidemiology and genetics of rheumatoid arthritis. Arthritis Res 2002;4(Suppl 3):S265-S272. https://doi.org/10.1186/ar578
2. Bläss S, Engel JM, Burmester GR. The immunologic homunculus in rheumatoid arthritis. Arthritis Rheum 1999;42:2499-2506. https://doi.org/10.1002/1529-0131(199912)42:12<2499::AID-ANR1>3.0.CO;2-R
3. Edwards RR, Wasan AD, Bingham CO 3rd, Bathon J, Haythornthwaite JA, Smith MT, Page GG. Enhanced reactivity to pain in patients with rheumatoid arthritis. Arthritis Res Ther 2009;11:R61. https://doi.org/10.1186/ar2684
4. Rittner HL, Mousa SA, Labuz D, Beschmann K, Schäfer M, Stein C, Brack A. Selective local PMN recruitment by CXCL1 or CXCL2/3 injection does not cause inflammatory pain. J Leukoc Biol 2006;79:1022-1032. https://doi.org/10.1189/jlb.0805452
5. Cunha TM, Verri WA Jr, Schivo IR, Napimoga MH, Parada CA, Poole S, Teixeira MM, ET AL. Crucial role of neutrophils in the development of mechanical inflammatory hypernociception. J Leukoc Biol 2008;83:824-832. https://doi.org/10.1189/jlb.0907654
6. Pelletier M, Maggi L, Micheletti A, Lazzeri E, Tamassia N, Costantini C, Cosmi L, ET AL. Evidence for a cross-talk between human neutrophils and Th17 cells. Blood 2010;115:335-343. https://doi.org/10.1182/blood-2009-04-216085
7. Wang CH, Dai JY, Wang L, Jia JF, Zheng ZH, Ding J, Chen Z-N, Zhu P. Expression of CD147 (EMMPRIN) on neutrophils in rheumatoid arthritis enhances chemotaxis, matrix metalloproteinase production and invasiveness of synoviocytes. J Cell Mol Med 2011;15:850-860. https://doi.org/10.1111/j.1582-4934.2010.01084.x

8. Kumar S, Gupta E, Kaushik S, Jyoti A. Neutrophil Extracellular Traps: Formation and Involvement in Disease Progression. Iran J Allergy Asthma Immunol 2018;17:208-220.
9. Willis VC, Banda NK, Cordova KN, Chandra PE, Robinson WH, Cooper DC, ET AL. Protein arginine deiminase 4 inhibition is sufficient for the amelioration of collagen-induced arthritis. Clin Exp Immunol 2017;188:263-274. https://doi.org/10.1111/cei.12932
10. Villanueva E, Yalavarthi S, Berthier CC, Hodgin JB, Khandpur R, Lin AM, Rubin CJ, ET AL. Netting neutrophils induce endothelial damage, infiltrate tissues, and expose immunostimulatory molecules in systemic lupus erythematosus. J Immunol 2011;187:538-552. https://doi.org/10.4049/jimmunol.1100450
11. Jorch SK, Kubes P. An emerging role for neutrophil extracellular traps in noninfectious disease. Nat Med 2017;23:279-287. https://doi.org/10.1038/nm.4294
12. Wang Y, Catana F, Yang Y, Roderick R, van Breemen RB. An LC-MS method for analyzing total resveratrol in grape juice, cranberry juice, and in wine. J Agric Food Chem 2002;50:431-435. https://doi.org/10.1021/jf010812u
13. Wei Y, Jia J, Jin X, Tong W, Tian H. Resveratrol ameliorates inflammatory damage and protects against osteoarthritis in a rat model of osteoarthritis. Mol Med Rep 2018;17:1493-1498. https://doi.org/10.3892/mmr.2017.8036
14. Rauf A, Imran M, Suleria HAR, Ahmad B, Peters DG, Mubarak MS. A comprehensive review of the health perspectives of resveratrol. Food Funct 2017;8:4284-4305. https://doi.org/10.1039/C7FO01300K
15. Nguyen C, Savouret JF, Widerak M, Corvol MT, Rannou F. Resveratrol, Potential Therapeutic Interest in Joint Disorders: A Critical Narrative Review. Nutrients 2017;9:45. https://doi.org/10.3390/nu9010045
16. Yang G, Chang CC, Yang Y, Yuan L, Xu L, Ho CT, Li S. Resveratrol Alleviates Rheumatoid Arthritis via Reducing ROS and Inflammation, Inhibiting MAPK Signaling Pathways, and Suppressing Angiogenesis. J Agric Food Chem 2018;66:12953-12960. https://doi.org/10.1021/acs.jafc.8b05047
17. Khojah HM, Ahmed S, Abdel-Rahman MS, Elhakeim EH. Resveratrol as an effective adjuvant therapy in the management of rheumatoid arthritis: a clinical study. Clin Rheumatol 2018;37:2035-2042. https://doi.org/10.1007/s10067-018-4080-8
18. Pinto LG, Talbot J, Peres RS, Franca RF, Ferreira SH, Ryffel B, Aves-Filho CF, ET AL. Joint production of IL-22 participates in the initial phase of antigen-induced arthritis through IL-1β production. Arthritis Res Ther 2015;17:235. https://doi.org/10.1186/s13075-015-0759-2
19. Pinto LG, Cunha TM, Vieira SM, Lemos HP, Verri WA, Cunha FQ, Ferreira SH. IL-17 mediates articular hypernociception in antigen-induced arthritis in mice. Pain 2010;148:247-256. https://doi.org/10.1016/j.pain.2009.11.006
20. Cunha TM, Verri WA, Silva JS, Poole S, Cunha FQ, Ferreira SH. A cascade of cytokines mediates mechanical inflammatory hypernociception in mice. Proc Natl Acad Sci U S A 2005;102:1755-1760. https://doi.org/10.1073/pnas.0409225102
21. Krautgartner WD, Klappacher M, Hannig M, Obermayer A, Hartl D, Marcos V, Vitkov L. Fibrin mimics neutrophil extracellular traps in SEM. Ultrastruct Pathol 2010;34:226-231. https://doi.org/10.3109/01913121003725721
22. Caudrillier A, Kessenbrock K, Gilliss BM, Nguyen JX, Marques MB, Monestier M, Toy P, ET AL. Platelets induce neutrophil extracellular traps in transfusion-related acute lung injury. J Clin Invest 2012;122:2661-2671. https://doi.org/10.1172/JCI61303
23. Lefrançais E, Mallavia B, Zhuo H, Calfee CS, Looney MR. Maladaptive role of neutrophil extracellular traps in pathogen-induced lung injury. JCI Insight 2018;3:e98178. https://doi.org/10.1172/jci.insight.98178
24. Wang B, Bellot GL, Iskandar K, Chong TW, Goh FY, Tai JJ, Schwarz H, ET AL. Resveratrol attenuates TLR-4 mediated inflammation and elicits therapeutic potential in models of sepsis. Sci Rep 2020;10:18837. https://doi.org/10.1038/s41598-020-74578-9
25. Khandpur R, Carmona-Rivera C, Vivekanandan-Giri A, Gizinski A, Yalavarthi S, Knight JS, Frisay S, ET AL. NETs are a source of citrullinated autoantigens and stimulate inflammatory responses in rheumatoid arthritis. Sci Transl Med 2013;5:178ra40. https://doi.org/10.1126/scitranslmed.3005580
26. Royzman D, Andreev D, Stich L, Rauh M, Bäuerle T, Ellmann S, Boon L, ET AL. Soluble CD83 Triggers Resolution of Arthritis and Sustained Inflammation Control in IDO Dependent Manner. Front Immunol 2019;10:633. https://doi.org/10.3389/fimmu.2019.00633

27. Claushuis TAM, van der Donk LEH, Luitse AL, van Veen HA, van der Wel NN, van Vught LA, Roelofs JJTH, ET AL. Role of Peptidylarginine Deiminase 4 in Neutrophil Extracellular Trap Formation and Host Defense during Klebsiella pneumoniae-Induced Pneumonia-Derived Sepsis. J Immunol 2018;201:1241-1252. https://doi.org/10.4049/jimmunol.1800314
28. Breuss J, Atanasov A, Uhrin P. Resveratrol and Its Effects on the Vascular System. IJMS 2019;20:1523. https://doi.org/10.3390/ijms20071523
29. Rauf A, Imran M, Butt MS, Nadeem M, Peters DG, Mubarak MS. Resveratrol as an anti-cancer agent: A review. Critical Reviews in Food Science and Nutrition 2018;58:1428-1447. https://doi.org/10.1080/10408398.2016.1263597
30. Nunes S, Danesi F, Del Rio D, Silva P. Resveratrol and inflammatory bowel disease: the evidence so far. Nutr Res Rev 2018;31:85-97. https://doi.org/10.1017/S095442241700021X
31. Alesci A, Nicosia N, Fumia A, Giorgianni F, Santini A, Cicero N. Resveratrol and Immune Cells: A Link to Improve Human Health. Molecules 2022;27:424. https://doi.org/10.3390/molecules27020424
32. Ravindran M, Khan MA, Palaniyar N. Neutrophil Extracellular Trap Formation: Physiology, Pathology, and Pharmacology. Biomolecules 2019;9:365. https://doi.org/10.3390/biom9080365
33. De Souza Andrade MM, Leal VNC, Fernandes IG, Gozzi-Silva SC, Beserra DR, Oliveira EA, Teixeira FME, ET AL. Resveratrol Downmodulates Neutrophil Extracellular Trap (NET) Generation by Neutrophils in Patients with Severe COVID-19. Antioxidants (Basel) 2022;11:1690. https://doi.org/10.3390/antiox11091690
34. Schuligoi R, Amann R, Prenn C, Peskar BA. Effects of the cyclooxygenase-2 inhibitor NS-398 on thromboxane and leukotriene synthesis in rat peritoneal cells. Inflamm Res 1998;47:227-230. https://doi.org/10.1007/s000110050321
35. Sinatra R. Role of COX-2 inhibitors in the evolution of acute pain management. J Pain Symptom Manage 2002;24(1 Suppl):S18-S27. https://doi.org/10.1016/S0885-3924(02)00410-4
36. Zhang J, Song X, Cao W, Lu J, Wang X, Wang G, Wang Z, Chen X. Autophagy and mitochondrial dysfunction in adjuvant-arthritis rats treatment with resveratrol. Sci Rep 2016;6:32928. https://doi.org/10.1038/srep32928
37. Riveiro-Naveira RR, Valcárcel-Ares MN, Almonte-Becerril M, Vaamonde-García C, Loureiro J, Hermida-Carballo L, López-Peláez E, ET AL. Resveratrol lowers synovial hyperplasia, inflammatory markers and oxidative damage in an acute antigen-induced arthritis model. Rheumatology (Oxford) 2016;55:1889-1900. https://doi.org/10.1093/rheumatology/kew255
38. Kirchner T, Hermann E, Möller S, Klinger M, Solbach W, Laskay T, Behnen M. Flavonoids and 5-Aminosalicylic Acid Inhibit the Formation of Neutrophil Extracellular Traps. Mediators Inflamm 2013;2013:710239. https://doi.org/10.1155/2013/710239
39. Jablonska E, Garley M, Surazynski A, Grubczak K, Iwaniuk A, Borys J, Moniuszko M, Ratajczak-Wrona W. Neutrophil extracellular traps (NETs) formation induced by TGF-β in oral lichen planus - Possible implications for the development of oral cancer. Immunobiology 2020;225:151901. https://doi.org/10.1016/j.imbio.2019.151901
40. Simmonds RE, Foxwell BM. Signalling, inflammation and arthritis: NF-kappaB and its relevance to arthritis and inflammation. Rheumatology (Oxford) 2008;47:584-590. https://doi.org/10.1093/rheumatology/kem298
41. Lu J, Zheng Y, Yang J, Zhang J, Cao W, Chen X, Fang S. Resveratrol alleviates inflammatory injury and enhances the apoptosis of fibroblast-like synoviocytes via mitochondrial dysfunction and ER stress in rats with adjuvant arthritis. Mol Med Rep 2019;20:463-472. https://doi.org/10.3892/mmr.2019.10273
42. Yang CM, Chen YW, Chi PL, Lin CC, Hsiao LD. Resveratrol inhibits BK-induced COX-2 transcription by suppressing acetylation of AP-1 and NF-κB in human rheumatoid arthritis synovial fibroblasts. Biochem Pharmacol 2017;132:77-91. https://doi.org/10.1016/j.bcp.2017.03.003